Available online at www.sciencedirect.com

SciVerse ScienceDirect

Ceramics International 39 (2013) 8493–8498

CERAMICS INTERNATIONAL

www.elsevier.com/locate/ceramint

Short communication

Development of SiO_2 based thin film on metal foils for space application

I. Neelakanta Reddy[a,b], V. Rajagopal Reddy[b], N. Sridhara[a], S. Basavaraja[c], M. Venkatanarayana[a], V. Sasidhara Rao[a], A.K. Sharma[a], Arjun Dey[a,*]

[a]*Thermal Systems Group, ISRO Satellite Centre, Vimanapura Post, Bangalore 560 017, India*
[b]*Department of Physics, Sri Venkateswara University, Tirupati 517502, India*
[c]*Bruker India Nanotechnology Laboratory, Jawaharlal Nehru Centre for Advanced Scientific Research (JNCASR), Jakkur, Bangalore 560064, India*

Received 7 January 2013; received in revised form 28 January 2013; accepted 25 February 2013
Available online 6 March 2013

Abstract

Silica (SiO_2) mono-layer and silica–alumina (SiO_2–Al_2O_3) bi-layer thin films were developed on both SS304 and Ti thin foils by pulsed rf magnetron sputtering. The solar absorptance (α_s) and IR emittance (ε_{ir}) of the films were measured. Both α_s and ε_{ir} of SS304 and Ti were increased after depositing SiO_2 and SiO_2–Al_2O_3 bi-layer thin film. The ratio of solar absorptance and IR emittance (i.e. $\alpha_s/\varepsilon_{ir}$) can be tailored in a large range e.g. 3.3–0.850 for SS and 3.66–1.085 for Ti which is useful for many spacecraft subsystems to tailor their operating temperatures. Further, the microstructure, surface morphology and topography of the films were investigated by field emission scanning electron microscopy, energy dispersive X-ray spectroscopy and atomic force microscopy.

Keywords: B. Microstructure; C. Solar absorptance; C. IR emittance; D. SiO_2–Al_2O_3; Thin film; Rf magnetron sputtering

1. Introduction

In space missions metallic thin foils made of Ti, SS and Ta are often employed as heat shields to protect the adjacent subsystems from high flux of propulsion flume. High emittance coatings on such metallic shields are required to improve their heat radiation characteristics. High emittance coatings help in maintaining the critical temperature level of spacecraft subsystems by rejecting the excess heat to space [1]. Oxide and carbide based high emittance thin films/coatings have been developed on various substrates [2–7]. Studies on SiO_2 based thin films have been reported for applications like semiconductors, opto-electronics, solar cells, due to their inherent anti-reflective, high-transmittance and good dielectric properties [10–15]. SiO_2 based composite films have potential of providing high emittance coating with high temperature withstanding properties [4,8,9]. However, the detailed investigation on this application is yet to be explored. In space missions where radiation is the predominant mode of heat transfer, development of high emittance thin films on metallic substrates for thermal control application is of paramount importance.

The present communication describes the studies related to the development of SiO_2 and SiO_2–Al_2O_3 film on SS304 and Ti substrates using pulsed rf magnetron sputtering. Process optimization was carried out with respect to suitable solar absorptance and IR emittance ($\alpha_s/\varepsilon_{ir}$) ratio for spacecraft thermal control application. Further, microstructure and surface morphology of the film were examined.

2. Materials and methods

SiO_2 mono-layer and SiO_2–Al_2O_3 bi-layer films were deposited on SS304 and Ti (99.9%, B&S Aircraft Alloy Inc. USA) foils thickness of 75 μm by pulsed rf magnetron sputtering (SD20, Scientific Vacuum Systems, UK) at room temperature (25 ± 2 °C). Both, SiO_2 and Al_2O_3 targets (dia-8″, thickness- 6 mm and purity better than 99.99%) were

*Corresponding author. Tel.: +91 8025083214.
E-mail addresses: arjundey@isac.gov.in, arjun_dey@rediffmail.com (A. Dey).

0272-8842/$ - see front matter © 2013 Elsevier Ltd and Techna Group S.r.l. All rights reserved.
http://dx.doi.org/10.1016/j.ceramint.2013.02.082

obtained from Soleras Ltd, USA. Prior to sputtering, substrates were ultrasonically cleaned by GR grade isopropyl alcohol (Merck, India). Further, SS304 substrate was cleaned using 60% (V/V) sulfuric acid and Ti substrates using 70% (V/V) nitric acid for 5 min. This was followed by drying in hot air oven (UT6060, Heraeus, Germany) at 120 °C for 15 min. The sputtering chamber was evacuated to an ultimate pressure of 5.0×10^{-6} mbar using a combination of rotary pump (D40B, Oerlikon Leybold Vacuum, Germany) and turbo molecular pump (1000C, Oerlikon Leybold Vacuum, Germany). Sputtering chamber was maintained at a working pressure of 1.5×10^{-2} mbar during deposition by allowing the argon gas (99.999%). Prior to deposition, SiO_2 and Al_2O_3 targets were pre-sputtered for 20 min to remove contamination on the surface, if any. SiO_2 films were deposited at a constant rf power of 400 W for the duration of 2 h to 24 h. Further, an Al_2O_3 layer was deposited on corresponding SiO_2 layers at a constant rf power of 700 W for a fixed time of 7 h. The suitable parameters e.g. rf power and deposition time of Al_2O_3 layer were judiciously chosen on the basis of good adhesion.

2.1. Characterization of the film

The adhesion test was carried out by utilizing 'Tape ($\sim 25 \times 10^{-3}$ m width, 3 M-250, 3 M, USA) Peel Method' as per ASTM D903 [16].

The α_s and ε_{ir} of the deposited films were measured at room temperature and ambient humid condition by solar spectrum reflectometer (SSR-E, Devices and Services Co., USA) and emissometer (AE, Devices and Services Co., USA), respectively. Calibration of the solar spectrum reflectometer was performed by the standards provided by machine supplier for the high reflectance (0.886) and black body reflectance (0). Further, calibration of the emissometer was performed by the standards provided by machine supplier for the high emittance (0.88) as well as low emittance (0.05) before measurements. An average α_s and ε_{ir} data can be obtained digitally from the aforesaid instruments over entire solar or IR spectrum region. Further, α_s and ε_{ir} data was reported in the present study with an average of at least five readings with an error of 1–3%.

Further, for thickness measurement and coating-substrate interface investigation, field emission scanning electron microscopy (FE-SEM: Supra VP35 Carl Zeiss, Germany) was utilized. The cross-sections of the coatings were cold mounted and polished with diamond paste (Eastern Diamond Products Pvt. Ltd., Kolkata, India) of 0.25 μm grit size and finally with an alumina suspension (average particle size, d_{50}–0.03 μm). Elemental line profile analysis of the deposited films was carried out by energy dispersive X-ray (EDX: X-Max, Oxford Instruments, UK) spectroscopy. Atomic force microscopy (AFM: diInnova, Bruker, USA) was also employed to investigate the surface morphology and roughness of the films. The etched silicon cantilever probes (RTESP, Bruker, USA) of 125 μm were used at a drive frequency of ~260–320 kHz. A first order flattening was done for all the AFM images for optimum clarity in visual presentation.

3. Results and discussions

The SiO_2 mono-layer and SiO_2–Al_2O_3 bi-layer films showed excellent adhesion with both the metal substrates e.g., SS304 and Ti. No peel off or damage on the coating surfaces was observed after the tape peel adhesion test carried out as per ASTM D903.

The variation of α_s, ε_{ir} and the ratio of α_s and ε_{ir} as a function of deposition time of SiO_2 on both SS304 and Ti are shown in Fig. 1a–c, respectively.

The α_s of bare SS304 and Ti thin foils were measured as 0.33 and 0.53, respectively. It was increased to ~0.59 (for SS) and ~0.76 (for Ti) after deposition of SiO_2 for 24 h. The α_s was almost unchanged introducing mono-layer of Al_2O_3 on SiO_2, except for 12 h. Similarly, the ε_{ir} of bare SS304 and Ti thin foils were measured as 0.12 (for SS) and 0.16 (for Ti), respectively. After 24 h deposition of SiO_2 layer, ε_{ir} of both the substrates increased to ~0.7. Further, Al_2O_3 layer on SiO_2 gave a sharp increase of ε_{ir} value for the corresponding SiO_2 layer from 8 to 12 h. The increase in ε_{ir} with SiO_2–Al_2O_3 bi-layer combination was 68% vs. 19% that with the corresponding mono-layer of SiO_2. However, after 12 h deposition time of SiO_2, ε_{ir} increased very sluggishly. Further, at 24 h, SiO_2–Al_2O_3 bi-layer showed marginally lower ε_{ir} than that of corresponding SiO_2 mono-layer. The corresponding ratio of α_s and ε_{ir} was ~3.3 for both the bare metal substrates. Initially, 2 h deposition of SiO_2 on SS showed $\alpha_s/\varepsilon_{ir}$ value of 2.75, afterwards it was decreased up to 0.85 after 24 h of deposition. However, Al_2O_3 on corresponding SiO_2 layer of 8 h showed $\alpha_s/\varepsilon_{ir}$ value of 1.53 which dropped sharply to 0.94 and from 12 h to 24 h it almost remain constant. Similarly, $\alpha_s/\varepsilon_{ir}$ increased initially from 3.31 to 3.66 after 2 h of SiO_2 deposition on Ti, afterwards, it was decreased to 1.08 after 24 h deposition of SiO_2. However, Al_2O_3 on corresponding SiO_2 layer of 8 h showed $\alpha_s/\varepsilon_{ir}$ value of 2.69 which dropped sharply to 1.15 at 12 h and was remaining almost constant up to 24 h.

It may be concluded from the data presented in Fig. 1c that after 12 h deposition of SiO_2 the variation of $\alpha_s/\varepsilon_{ir}$ was almost insignificant. Therefore, further increase in thickness (i.e. deposition time as the thickness is directly proportional to the deposition time) of SiO_2 layer beyond 12 h did not affect the thermo-optical properties of the surface. The combination of Al_2O_3 layer with SiO_2 layer deposited for 12 h showed an optimized condition because further increase in deposition time (i.e. increase in thickness) did not show any significant deviation of α_s, ε_{ir}, as well as $\alpha_s/\varepsilon_{ir}$.

The SiO_2 film thickness of 3.75 μm on aluminum by evaporation method showed ε_{ir} value of 0.55 [9], whereas SiO_2 film thickness of 2.2 μm on copper–indium–gallium–diselenide solar cell gave ε_{ir} value of 0.65 [4]. An additional Al_2O_3 layer and a total layer thickness of 2.5 μm offered further increase of ε_{ir} to 0.77. The comparable ε_{ir} values were also achieved in the present case. However, in the present work, both thicknesses of mono-layer of SiO_2 and bi-layer of

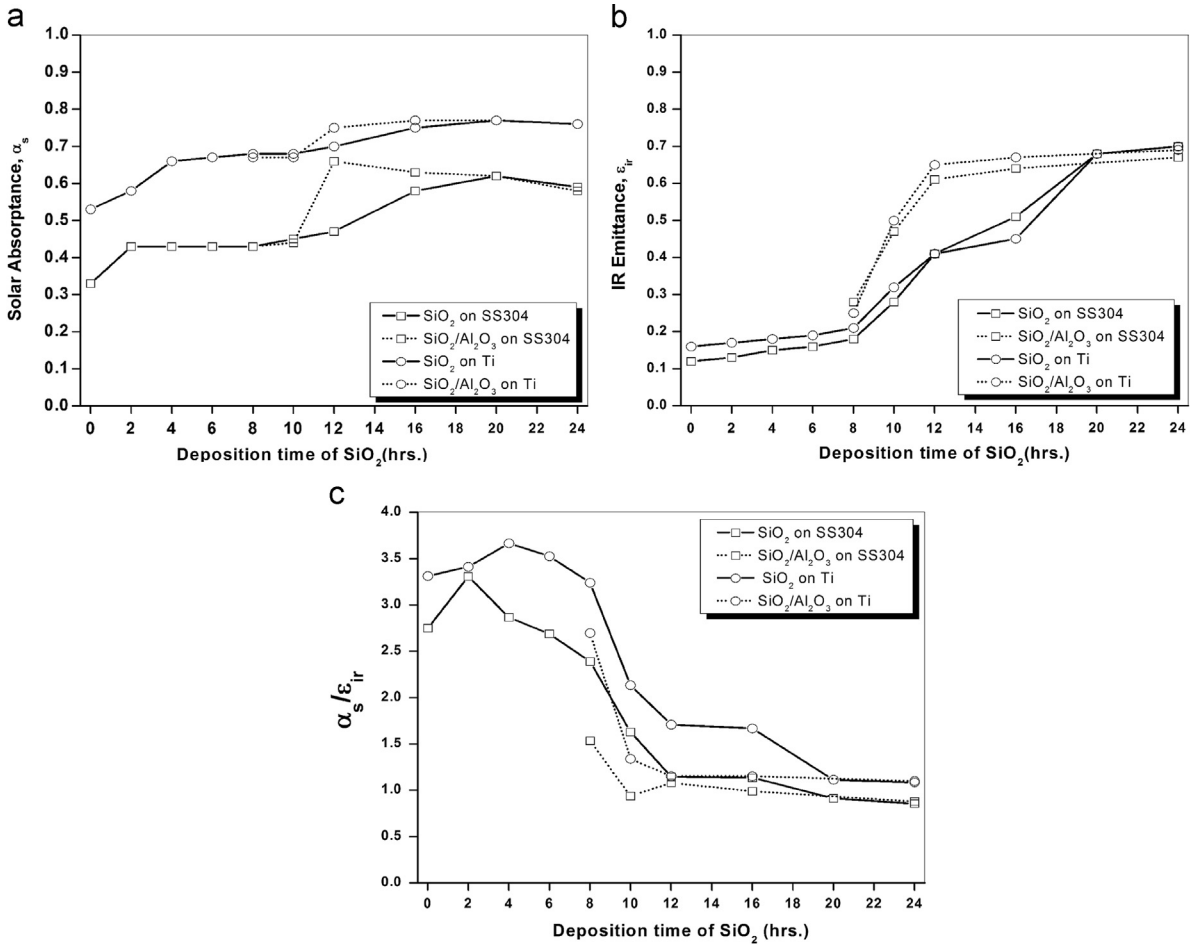

Fig. 1. Variation of (a) solar absorptance, (b) IR emittance and (c) ratio of solar absorptance and IR emittance as a function of deposition time of SiO_2 on both SS304 and Ti substrates (dotted line represents the data of Al_2O_3 coating at a constant deposition time of 7 h on corresponding SiO_2 layer).

SiO_2–Al_2O_3 on SS and Ti were much lesser than reported values [3,9].

In space; radiation is the predominant mode of heat transfer. The steady-state temperature of any system or spacecraft excluding internal heat dissipation, if any can be expressed by the following relation [17]:

$$T_{abs} = \left(\frac{SA_p\alpha_s}{\sigma A_t \varepsilon_{ir}}\right)^{1/4} \quad (1)$$

where 'T_{abs}' is the absolute temperature of the spacecraft, 'S' is the solar constant of 1353 W m^{-2} and σ is Stefan–Boltzmann constant of 56.7×10^{-9} W m^{-2} K^{-1}. 'A_p' is the projected specified surface area perpendicular to the solar rays and 'A_t' is the total surface area of the spacecraft or subsystem. Here, we assume 'A_p/A_t' as unity and the surface is isolated on one side and the other side is exposed to the space. The 'α_s' and 'ε_{ir}' are the solar absorptance of the specified surface of projected area and IR emittance of the exposed surface to the space, respectively. From the above relationship one can understand that the temperature of the spacecraft or subsystem is controlled by only $\alpha_s/\varepsilon_{ir}$, as other parameters in the Eq. (1) are constants for a steady state condition.

Further, this model was applied to the present work to realize how '$\alpha_s/\varepsilon_{ir}$' value can affect the temperature of the spacecraft. The reduction of surface temperature can be achieved after introducing a SiO_2 mono-layer and SiO_2–Al_2O_3 bi-layer on SS and Ti as $\alpha_s/\varepsilon_{ir}$ was decreased. Therefore, tailoring $\alpha_s/\varepsilon_{ir}$ is achievable with suitable combination of thickness of SiO_2 and Al_2O_3. This will facilitate in achieving the desirable operating temperature range of spacecraft subsystem. The '$\alpha_s/\varepsilon_{ir}$' of bare SS and Ti substrate were 2.75 and 3.31, respectively. This indicates an absorbing surface. Introducing SiO_2–Al_2O_3 film, the emittance was increased and thereby the ratio was reduced from 0.85 to 1.085 for the respective substrates.

Therefore, it was noticed from preceding discussion and experimental data that the bi-layer i.e. SiO_2 deposited for 12 h and Al_2O_3 deposited for 7 h showed an optimum combination to decrease '$\alpha_s/\varepsilon_{ir}$' resulting in reducing the surface temperature. Typical FE-SEM photomicrograph of the cross-section of SiO_2 thin film deposited for 12 h on SS304 with a thickness of ~925 nm is shown in Fig. 2a. A smooth interface between SiO_2 film and substrates (SS and Ti) resulted into a good adhesion [14]. Typical FE-SEM photomicrographs of cross-section of SiO_2–Al_2O_3 bi-layer film deposited for 12 h and 7 h on both SS304 and Ti are

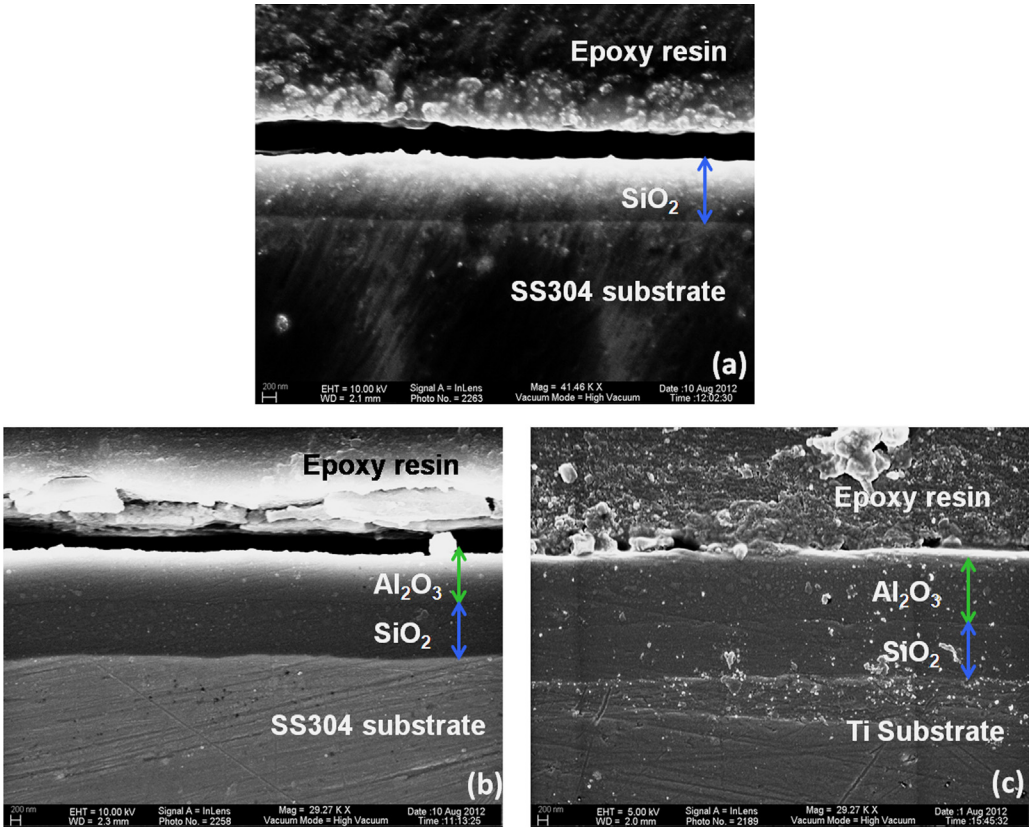

Fig. 2. Typical FE-SEM photomicrographs of cross section of the (a) SiO_2 mono-layer depositing for 12 h on SS304 substrate. SiO_2–Al_2O_3 bi-layers: SiO_2 depositing for 12 h and Al_2O_3 depositing for 7 h on (b) SS304 and (c) Ti substrate.

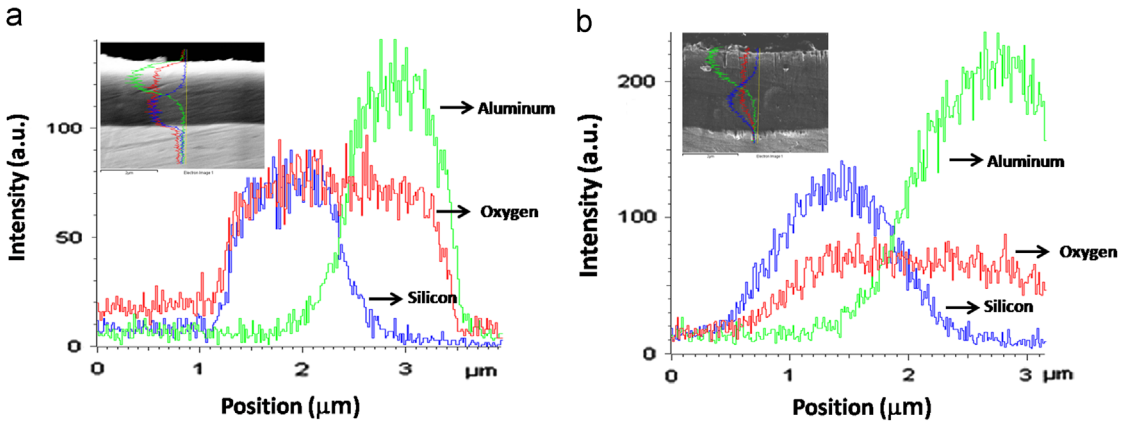

Fig. 3. Line profile EDX data of the cross-section of SiO_2–Al_2O_3 bi-layers on (a) SS304 and (b) Ti substrate (inset: corresponding cross-sectional FE-SEM image).

shown in Fig. 2b and c. The thickness of the Al_2O_3 layer was ~1000 nm. Good adhesion of the film revealed due to the smooth interface between SiO_2 and Al_2O_3. The standard deviation of the measured thickness data was less than 5%. Further, EDX line profile data of SiO_2–Al_2O_3 bi-layer coating on SS304 and Ti are shown in Fig. 3a and b, respectively. The data showed only the signature of silicon, aluminum and oxygen which are the elemental constituents of SiO_2 and Al_2O_3. A gradient interfacial diffusion of the silicon and aluminum ensured excellent adhesion between SiO_2 and Al_2O_3 layers.

The thickness was also measured from AFM photomicrographs by creating steps of individual layer of SiO_2 (deposited for 12 h) and Al_2O_3 (deposited for 7 h) on SS304 (Fig. 4a and b). The film thicknesses measured by AFM micrographs matched with FE-SEM data. AFM photomicrograph of the top surface of the 12 h deposited SiO_2 mono-layer are shown in Fig. 5a and b for SS304 and

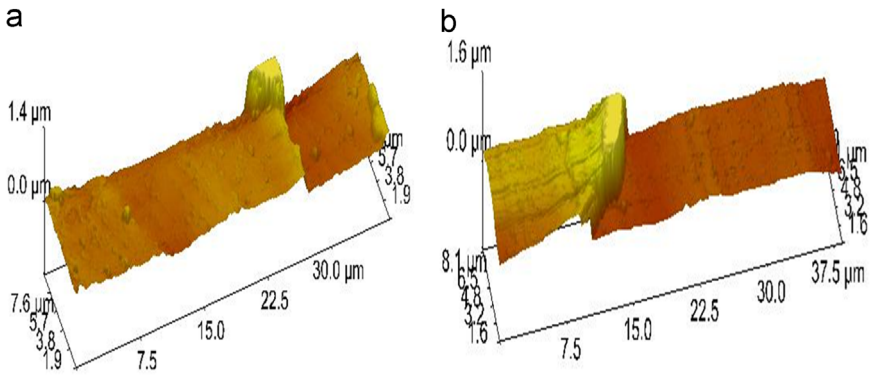

Fig. 4. AFM photomicrographs of the step of (a) SiO_2 and (b) Al_2O_3 mono-layers on SS304 substrate.

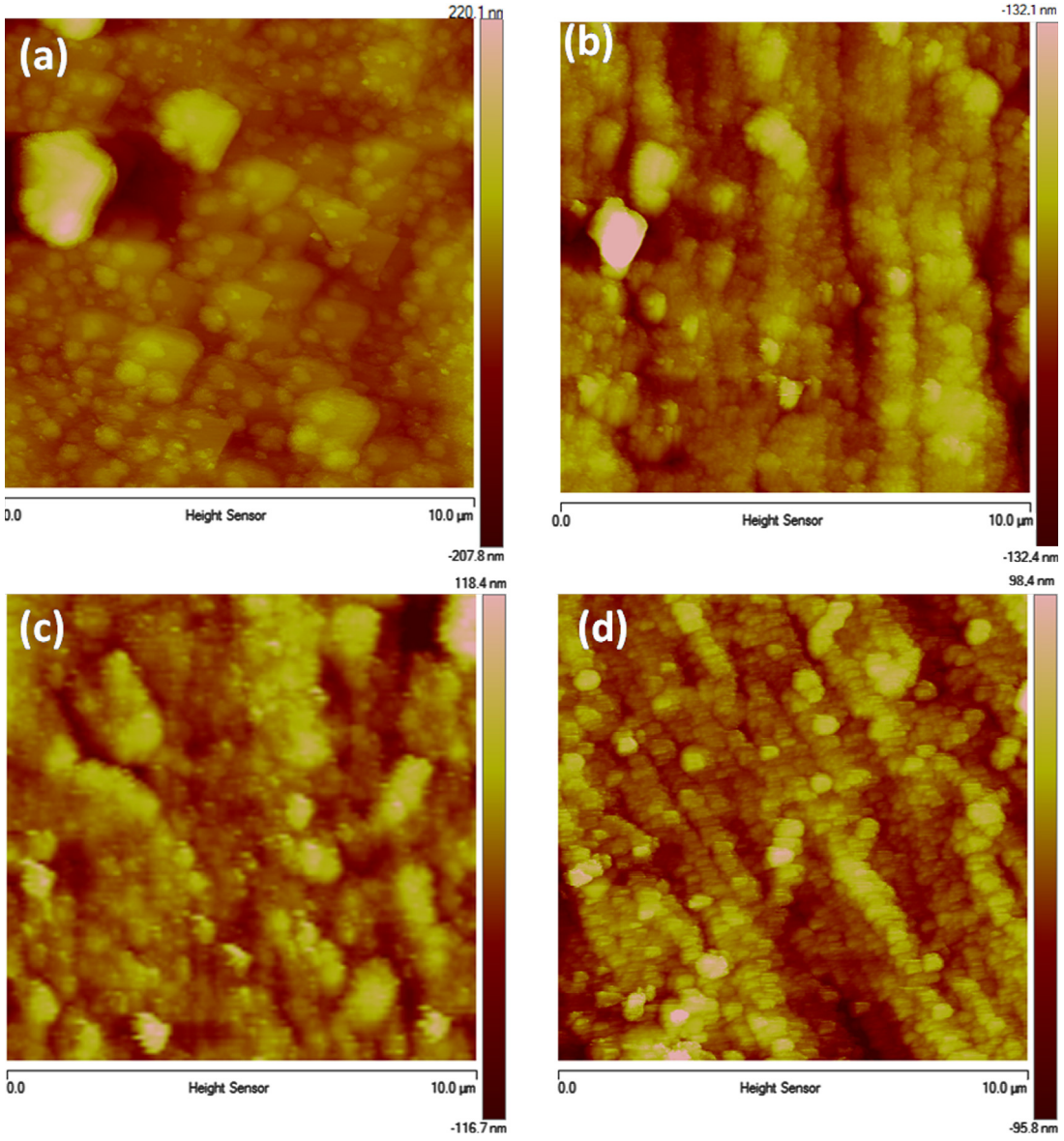

Fig. 5. AFM photomicrographs of the plan-section of SiO_2 mono-layer on (a) SS304 and (b) Ti substrate and Al_2O_3 mono-layer on (c) SS304 and (d) Ti substrate.

Ti substrate, respectively. Similarly, Al_2O_3 mono-layers on SS304 and Ti are shown in Fig. 5c and d, respectively. The dense distributions of nano-particles of spherical shape were observed for both individual SiO_2 and Al_2O_3 mono-layer as also reported by others [15]. The ranges of nano-particle size of SiO_2 and Al_2O_3 were 20–54 nm and 25–60 nm, respectively.

However, seldom agglomeration of nano-particles was observed in SiO_2 film. The R_a value of SiO_2 film was marginally increased e.g. 28.6 nm (vs. 25.7 nm) for SS and 24.5 nm (vs. 19.4 nm) for Ti than that of bare substrate. Similar trend of data was also observed for Al_2O_3 coating. The measured R_a values were 22 nm and 14 nm for SS and Ti substrate, respectively. The surface morphology of the SiO_2 and Al_2O_3 individual layer was similar to the reported data [18,19]. The R_a values reported [18,19] for both SiO_2 and Al_2O_3 thin films were much lesser than the present observation because highly polished non-metallic materials like Si, glass etc. were utilized as substrate.

4. Conclusions

Pulsed rf magnetron sputtering was employed to develop SiO_2 and SiO_2–Al_2O_3 coatings on SS304 and Ti foils. The deposition time of SiO_2 monolayer was varied from 2 h to 24 h. For SiO_2–Al_2O_3 bi-layer coating; the deposition time of SiO_2 was varied from 2 h to 24 h and thereafter Al_2O_3 was deposited for 7 h. Both the solar absoptance and infrared emittance values were increased after deposition of SiO_2 mono-layer and SiO_2–Al_2O_3 bi-layer films. However, the increase was predominant in infrared emittance ($\Delta\alpha_s \sim 0.25, \Delta\varepsilon_{ir} \sim 0.56$). The ratio of '$\alpha_s/\varepsilon_{ir}$', which is significant in a spacecraft thermal design can therefore be tailored in a wide range of 3.30–0.85 for SS and 3.66–1.09 for Ti substrate. The optimized SiO_2–Al_2O_3 coating was obtained by a combination of SiO_2 deposition for 12 h followed by Al_2O_3 deposition for 7 h. The corresponding thicknesses of SiO_2 and Al_2O_3 were ~925 nm and 1000 nm, respectively. Further increase in SiO_2 film thickness has not resulted into significant variation/ reduction in $\alpha_s/\varepsilon_{ir}$ ratio. FE-SEM cross section of the film showed a uniform deposition and smooth interfaces between SiO_2 and metal substrates and SiO_2 and Al_2O_3 layers. EDX elemental line profiles showed a gradient interfacial diffusion of Si and Al revealing a good adhesion between SiO_2 and Al_2O_3 bi-layer. AFM photomicrograph showed dense distribution of spherical shaped nano particles 20–54 nm for SiO_2 and 25–60 nm for Al_2O_3, respectively. R_a values were marginally increased after deposition of SiO_2 and Al_2O_3 films on the SS and Ti substrates.

References

[1] D.G. Gilmore (Ed.), Spacecraft thermal control handbook, The Aerospace corporation, California, 2002.

[2] F. Seronde, P. Echegut, J.P. Coutures, F. Gervais, Emissivity of oxides, a microscopic approach to glass coatings, Materials Science and Engineering B 8 (1991) 315–327.

[3] X. He, Y. Li, L. Wang, Y. Sun, S. Zhang, High emissivity coatings for high temperature application: progress and prospect, Thin Solid Films 517 (2009) 5120–5129.

[4] K. Shimazaki, M. Imaizumi, K. Kibe, SiO_2 and Al_2O_3/SiO_2 coatings for increasing emissivity of $Cu(In,Ga)Se_2$ thin-film solar cells for space applications, Thin Solid Films 516 (2008) 2218–2224.

[5] C. Siva Kumar, A.K. Sharma, K.N. Mahendra, S.M. Mayanna, Studies on anodic oxide coating with low absorptance and high emittance on aluminum alloy 2024, Solar Energy Materials and Solar Cells 60 (2000) 51–57.

[6] A.K. Sharma, H. Bhojraj, V.K. Kaila, H. Narayanamurthy, Anodizing and inorganic black colouring of aluminum alloys for space applications, Metal Finishing 95 (1997) 14–20.

[7] Y.M. Wang, H. Tian, X.E. Shen, L. Wen, J.H. Ouyang, Y. Zhou, D.C. Jia, L.X. Guo, An elevated temperature infrared emissivity ceramic coating formed on 2024 aluminum alloy by microarc oxidation, Ceramic International, 39 (2013) 2869–2875.

[8] J. Yi, X.D. He, Y. Sun, Y. Li, Electron beam-physical vapor deposition of SiC/SiO_2 high emissivity thin film, Applied Surface Science 253 (2007) 4361–4366.

[9] G. Hass, J.B. Ramsey, J.B. Heaney, J.J. Triolo, Reflectance, solar absorptivity, and thermal emissivity of SiO_2-coated aluminum, Applied Optics 8 (1969) 275–281.

[10] X. He, J. Wu, X. Li, X. Gao, L. Zhao, L. Wu, Synthesis and properties of silicon dioxide films prepared by pulsed laser deposition using ceramic SiO_2 target, Applied Surface Science 256 (2009) 231–234.

[11] H. Xiao, S. Huang, J. Zheng, G. Xie, Y. Xie, Optical characteristics of Si/SiO_2 multilayers prepared by magnetron sputtering, Microelectronic Engineering 86 (2009) 2342–2346.

[12] A. Barranco, F. Yubero, J. Cotrino, J.P. Espinos, J. Benıtez, T.C. Rojas, J. Allain, T. Girardeau, J.P. Riviere, A.R.G. Elipe, Low temperature synthesis of dense SiO_2 thin films by ion beam induced chemical vapor deposition, Thin Solid Films 396 (2001) 9–15.

[13] C. Yu, S. Zhu, D. Wei, F. Wang, Amorphous sol–gel SiO_2 film for protection of $Ti_6A_{l4}V$ alloy against high temperature oxidation, Surface and Coatings Technology 201 (2007) 5967–5972.

[14] F. Zhang, H. Zhu, W. Yang, Z. Wu, H. Qi, H. He, Z. Fan, J. Shao, Al_2O_3/SiO_2 films prepared by electron-beam evaporation as UV antireflection coatings on 4H–SiC, Applied Surface Science 254 (2008) 3045–3048.

[15] H.H. Huang, Y.S. Liu, Y.M. Chen, M.C. Huang, M.C. Wang, Effect of oxygen pressure on the microstructure and properties of the Al_2O_3–SiO_2 thin films deposited by E-beam evaporation, Surface and Coatings Technology 200 (2006) 3309–3313.

[16] N. Manavizadeh, F.A. Boroumand, E. Asl-Soleimani, F. Raissi, S. Bagherzadeh, A. Khodayari, M.A. Rasouli, Influence of substrates on the structural and morphological properties of rf sputtered ITO thin films for photovoltaic application, Thin Solid Films 517 (2009) 2324–2327.

[17] B.N. Agarwal, Design of geo-synchronous spacecraft, Prentice-Hall, NJ, 1986.

[18] J.N. Ding, X.F. Wang, N.Y. Yuan, C.L. Li, Y.Y. Zhu, B. Kan, The influence of substrate on the adhesion behaviours of atomic layer deposited aluminum oxide films, Surface and Coatings Technology 205 (2011) 2846–2851.

[19] S. Honda, M. Hirata, M. Ishimaru, Tunneling magneto resistance of ultra-thin Co–SiO_2 granular films with narrow current channels, Journal of Magnetism and Magnetic Materials 290–291 (2005) 1053–1055.